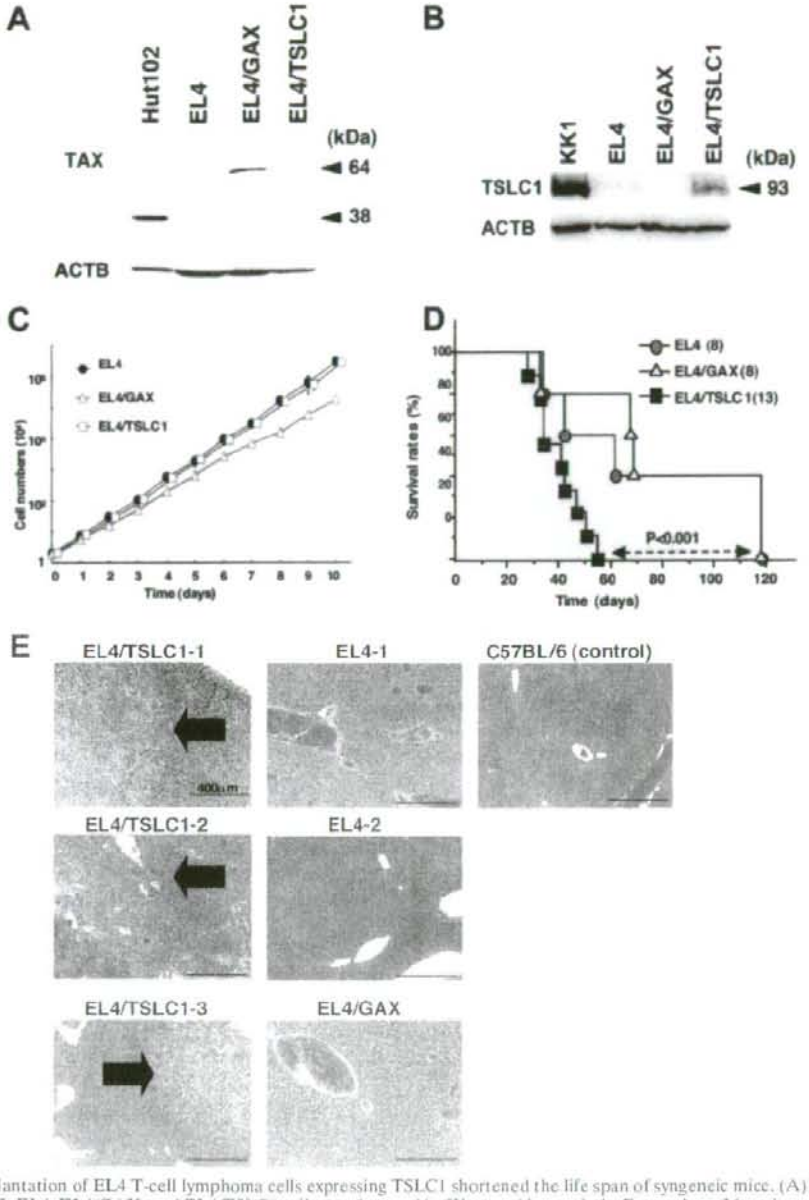

FIG. 1. Transplantation of EL4 T-cell lymphoma cells expressing TSLC1 shortened the life span of syngeneic mice. (A) Expression of Tax protein in HUT102, EL4, EL4/GAX, and EL4/TSLC1 cells was detected by Western blot analysis. Expression of β-actin protein (ACTB) was used as a loading control. (B) Expression of TSLC1 protein in KK1, EL4, EL4/GAX, and EL4/TSLC1 cells was detected by Western blot analysis. Expression of β-actin protein (ACTB) was used as a loading control. (C) Cell numbers in a growth curve are shown for an average of three independent counts, and standard deviations are indicated as error bars. (D) Survival curves of C57BL/6 mice inoculated in the abdominal cavity with EL4, EL4/GAX, or EL4/TSLC1 cells. Cumulative survival rates were calculated by the Kaplan-Meier method and compared using a log-rank test. (E) Liver sections from all mice were stained with hematoxylin-eosin. The regions of liver metastasis (arrow) were seen in liver sections from mice inoculated with EL4/TSLC1 cells but not shown in the liver sections from the mice inoculated with EL4 or EL4/GAX cells. Magnification, ×100; bars, 400 μm.

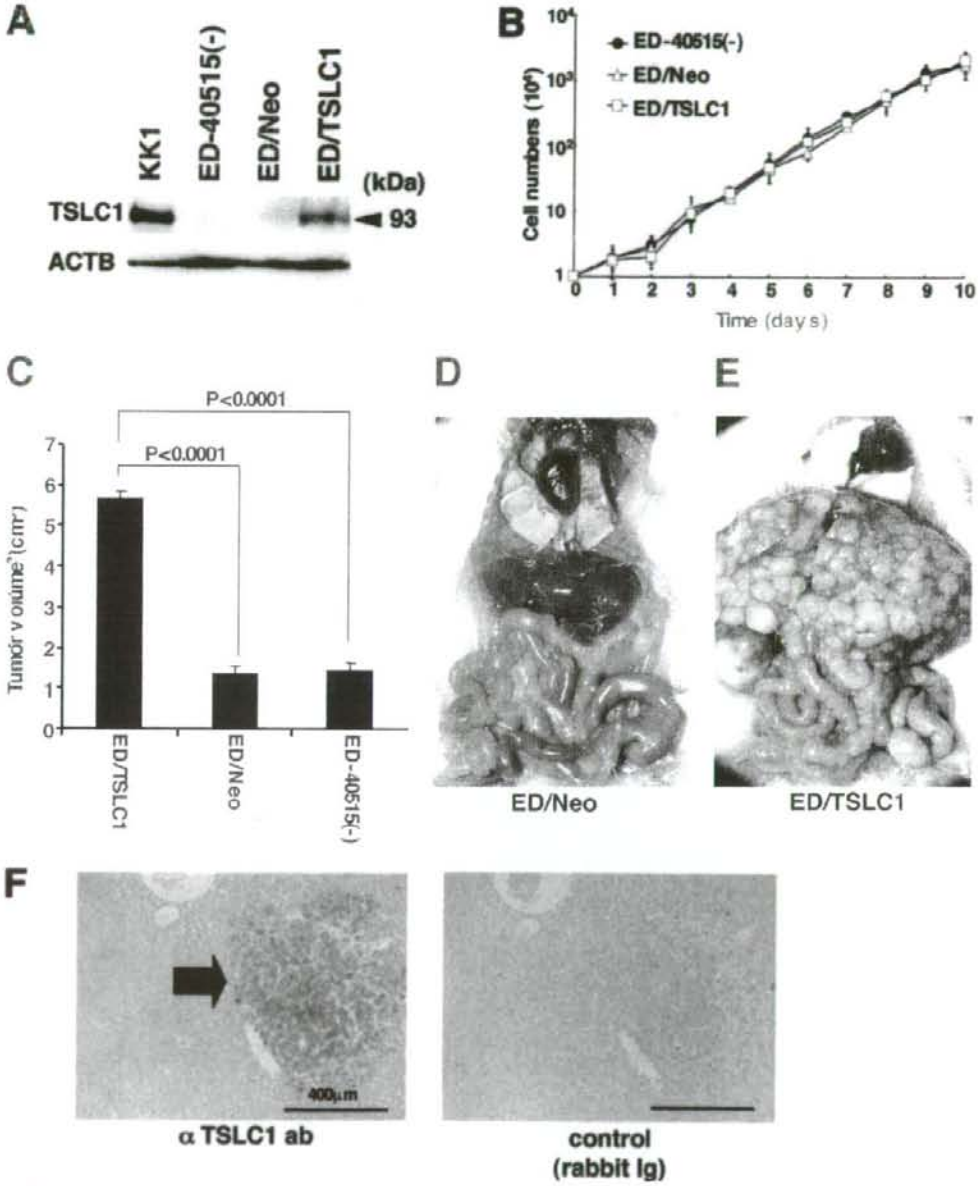

FIG. 2. Involvement of TSLC1 expression in tumor growth and infiltration of leukemia cells in NOG mice. (A) Expression of TSLC1 in KK1, ED-40515(−), ED/Neo, or ED/TSLC1 cell lines was detected by Western blot analysis. Expression of β-actin protein (ACTB) was used as a loading control. (B) Cell growth curves of ED-40515(−), ED/Neo, and ED/TSLC1 cell lines are shown for an average of three independent counts, and standard deviations are indicated as error bars. (C) Tumor volumes of mice inoculated subcutaneously with ED/TSLC1, ED/Neo, or ED-40515(−) cells after 21 days are shown as the means ± standard errors of the means for five mice in each group. Statistical analysis was done with a Student *t* test. (D and E) The pictures shown were derived from gross photographs of the sacrificed mice at 1 month after intravenous inoculation of ED/Neo (D) or ED/TSLC1 (E) cells. (F) Immunohistochemical staining for TSLC1 protein in liver metastases of the mice inoculated intravenously with ED/TSLC1 cells is shown. An arrow indicates a tumor mass with strong staining with a rabbit anti-TSLC1 antibody; however, the same mass shows no staining with rabbit immunoglobulin (Ig) as a negative control. Magnification, ×100; bars, 400 μm.

TABLE 1. Invasion scores of mice inoculated with ED/Neo or ED/TSLC1 cells

Cell line and mouse	Invasion score for organ by observation:									
	Macroscopic[a]					Microscopic[b]				
	Liver	Kidney	Lung	Ovary	Spleen	Liver	Kidney	Lung	Ovary	Spleen
ED/TSLC1										
T1	3+	−	+/−	1+	−	3−	−	2+	2+	−
T2	3+	−	−	1+	−	3−	−	2+	2+	−
T3	3+	−	+/−	2+	−	3−	−	2+	2+	−
T4	3+	−	−	1+	−	3+	−	2+	2+	−
T5	2+	−	−	2+	−	3+	−	2+	3+	−
T6	3+	−	+/−	1+	−	3+	−	+/−	2+	−
ED/Neo										
N1	−	−	−	2+	−	2+	−	+/−	3+	−
N2	+/−	−	−	1+	−	+/−	−	−	2+	−
N3	−	−	−	2+	−	−	−	+/−	2+	−
N4	−	−	−	1+	−	−	−	−	2+	−
N5	−	−	−	1+	−	ND[c]	ND	ND	ND	ND
N6	−	−	−	1+	−	ND	ND	ND	ND	ND

[a] Subjective invasion scores by macroscopic observation were as follows: −, no invasion; +/−, less than 10% invasion in the organ; 1+, 10 to 30% invasion in the organ; 2+, 30 to 70% invasion in the organ; 3+, over 70% invasion in the organ.

[b] Subjective invasion scores by microscopic observation were as follows: −, no invasion; +/−, less than 1% leukemia cells in the section; 1+, less than 10% leukemia cells in the section; 2+, 10 to 30% leukemia cells in the section; 3+, over 30% leukemia cells in the section.

[c] ND, not done.

detected by Western blot analysis (Fig. 1A). Expression of a TSLC1 protein in EL4/TSLC1 cells was also shown on Western blot analysis with KK1, an ATL cell line expressing TSLC1 (12) (Fig. 1B). In an in vitro cell growth assay, 2×10^4 cells were incubated, and their growth was analyzed by direct counting with trypan blue dye staining. EL4 and EL4/TSLC1 cells showed nearly identical proliferation profiles in vitro, while Tax-expressing EL4 cells proliferated more slowly (Fig. 1C). This difference in cell growth might be caused by different expression vectors. In an in vivo growth assay, 2×10^6 cells of each cell line were injected into the peritoneal cavity of C57BL/6J mice: eight mice for EL4 cells as controls, 13 mice for EL4/TSLC1 cells, and eight mice for EL4/GAX cells. All of the mice died of tumor invasion of various organs with ascitic fluids in 40 to 120 days. The median survival time of the control mice injected with EL4 cells or EL4/GAX cells was 72 days. The mice with EL4/TSLC1 cells, however, died within 60 days, with a median survival time of 41 days (Fig. 1D). The phenotypes of the control mice and the EL4/TSLC1 mice were almost identical with invasion of tumors into various organs. Organ metastasis of tumor cells in three EL4/TSLC1-inoculated mice, two EL4-inoculated mice, and one EL4/GAX-inoculated mouse was analyzed and evaluated with hematoxylin-eosin staining. The liver was one of the major sites of metastasis in all three of the EL4/TSLC1-inoculated mice by histopathological analysis but not in the two EL4-inoculated mice or the EL4/GAX-inoculated mouse (Fig. 1E). These results support the role of TSLC1 overexpression in T-lymphoma cells as one of an aggressive factor in the development of leukemia/lymphoma.

In order to investigate the possibility that overexpression of TSLC1 promotes tumor growth and/or infiltration in vivo,

TABLE 2. Clinical characteristics of patients and pathological findings of organ invasion[a]

Patient no.	Age (yr)/sex	Clinical characteristic				Invasion score in NOG mice[b]				TSLC1 expression score[c]
		Diagnosis (ATL type)	WBC (10^9/liter)	Lymphocytes (%)	Atypical cells (%)	Liver	Lung	Spleen	Lymph node	
1	73/M	Chronic	7.8	59	47	3+	3+	3+	ND	3+
2	59/F	Chronic	9.0	75	40	3+	2+	2+	1+	2+
3	66/F	Chronic	29.4	49	75	3+	3+	3+	ND	3+
4	44/F	Chronic	22.6	51	45	3+	2+	2+	2+	2+
5	43/F	Chronic	18.6	63	43	3+	3+	3+	ND	2+
6	54/M	Acute	192.8	65	91	1+	2+	ND	ND	1+
7	58/M	Acute	67.3	71	80	3+	3+	3+	ND	2+
8	65/F	Acute	29.4	25	60	3−	2+	ND	3+	3+
9	68/M	Acute	30.0	79	81	3+	1+	1+	2+	2+
10	66/F	Acute	10.2	38	51	3+	3+	3+	ND	3+

[a] Abbreviations: M, male; F, female; WBC, white blood cells; ND, not done.

[b] Subjective invasion scores were as follows: 0, no invasion; 1+, less than 10% leukemia cells in the section; 2+, 10 to 30% leukemia cells in the section; 3+, over 30% leukemia cells in the section.

[c] Subjective scores of TSLC1 expression in pathological immunostaining were as follows: −, no staining; 1+, faint staining in less than 10% of invasive leukemia cells; 2+, weak to moderate staining in 30 to 70% of invasive leukemia cells; 3+, intense staining in more than 70% of invasive leukemia cells.

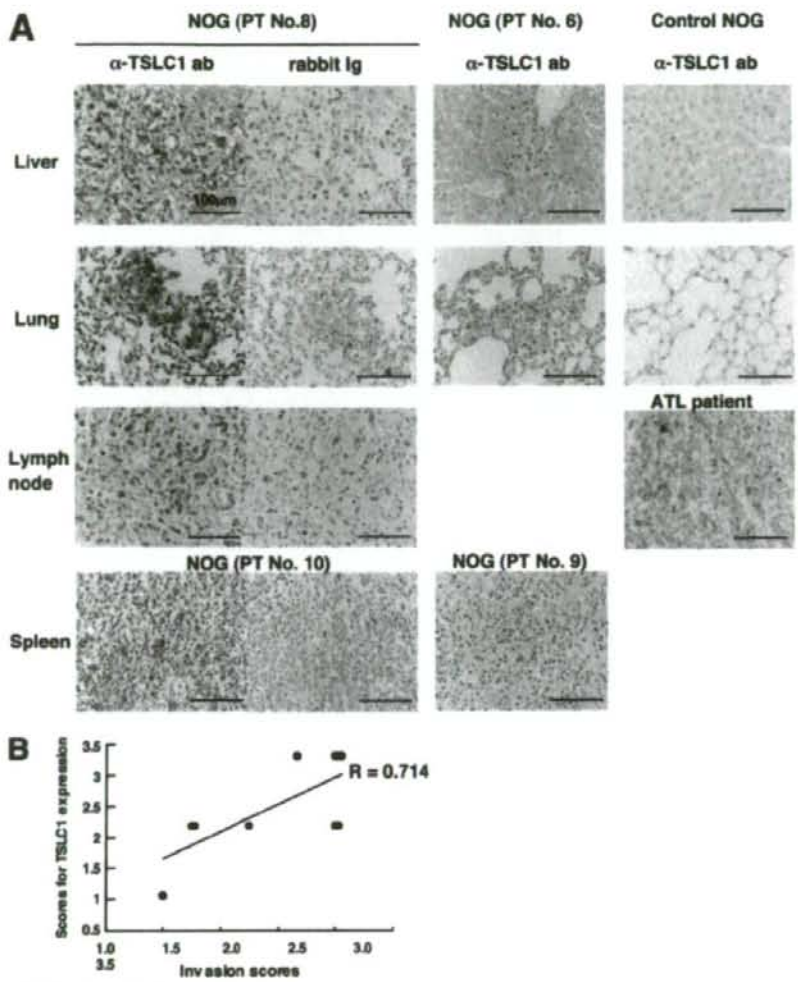

FIG. 3. Growth and infiltration of primary ATL cells in various organs of NOG mice based on TSLC1 expression. (A) Immunohistochemical staining of various organs of NOG mice inoculated with leukemia cells from patient 6, 8, 9, or 10 is shown with the use of rabbit anti-TSLC1 antibody or rabbit immunoglobulin (Ig) as a negative control. Sections from patients 8 and 10 showed severe invasion (invasion score, 3) and dense staining for TSLC1 (expression score, 3), while sections from patients 6 and 9 showed mild invasion (invasion score, 1) and light staining for TSLC1 (expression score, 1). Liver and lung sections from control NOG mice were used as negative controls, and a lymph node from an ATL patient was used as a positive control. Magnification, ×400; bars, 100 μm. (B) The diagram of dispersion between mean values of each invasion score and scores for TSLC1 expression in each NOG mouse inoculated with primary ATL cells showed moderate correlation ($R = 0.714$).

ATL-derived ED-40515(−) cells (10) were injected into NOG mice. Since expression of TSLC1 in ED-40515(−) cells is severely reduced by promoter methylation, they were transfected with either a TSLC1 expression plasmid (pcDNA3/TSLC1) or a mock plasmid (pcDNA3/Neo). ED/TSLC1 and ED/Neo cells were identified by selection with G-418. High levels of TSLC1 expression were verified in the ED/TSLC1 cells, but not in the ED/Neo cells, by Western blot analysis (Fig. 2A). The ED/TSLC1, ED/Neo, and ED-40515(−) cell lines all showed the same proliferation profile in vitro (Fig. 2B). Cells (10×10^6) were inoculated subcutaneously into the postauricular region of NOG mice, which permitted the observation of tumor growth macroscopically and the measurement of tumor size over a relatively short time (3). The ED/TSLC1 cell lines caused greater formation of larger tumors than did the ED/Neo and ED-40515(−) cell lines (Fig. 2C). The development of clinical signs of near-death (e.g., piloerection, weight loss, and cachexia) in mice at the time of killing was also more prevalent with the ED/TSLC1 cell line. These results suggest that TSLC1 expression in ATL cells enhances in vivo tumor growth in NOG mice.

Since the mice died within 4 weeks after subcutaneous in-

oculation of leukemia cells due to heavy tumor burden, 2×10^6 ED/TSLC1 or ED/Neo cells were intravenously injected into six NOG mice in order to investigate their capacity for invasion of various organs. After 1 month, we sacrificed the mice to determine the extent of organ invasion. Macroscopically, all of the mice injected with ED/TSLC1 cells (six/six) showed severe liver invasion with swelling of the ovaries. None of the mice injected with ED/Neo cells showed liver invasion, but they did show ovarian involvement (Fig. 2D and E). Microscopically, all of the mice inoculated with ED/TSLC1 cells showed severe and massive liver and lung invasions. On the other hand, only one of six mice inoculated with ED/Neo cells showed a large amount of liver metastasis (Table 1). TSLC1 expression in tumor cells infiltrating the liver was confirmed by immunohistochemical staining (Fig. 2F). Thus, overexpression of TSLC1 in ATL cells might enhance organ invasion, and particularly invasion of the liver and lung.

Next, we examined whether primary ATL cells with various levels of expression of TSLC1 could efficiently grow and infiltrate various organs in NOG mice. TSLC1-positive primary ATL cells (2×10^7) from five acute-type and five chronic-type ATL patients were inoculated subcutaneously into the postauricular region of NOG mice (Table 2). All of the mice developed clinical signs of near-death (e.g., piloerection, weight loss, and cachexia) 6 to 8 weeks after inoculation, in addition to the enlargement of the lymph nodes, spleen, lungs, and liver. Microscopically, ATL cells invaded various organs of all ATL-bearing NOG mice to different degrees. Based on results of immunohistochemical staining for TSLC1, all invading leukemia cells expressed TSLC1 protein, compared with no TSLC1 expression in these organs in control NOG mice (Table 2 and Fig. 3A). The dispersion diagram for the levels of invasion and the levels of TSLC1 expression in the leukemia cells showed a correlation coefficient of 0.714, suggesting that there was a moderate correlation between invasive capability and the level of TSLC1 expression (Fig. 3B). Thus, TSLC1 could aid in the formation of a rapidly growing large tumor and massive infiltration of ATL cells into various organs in NOG mice. Since TSLC1 is expressed in various types of ATL cells, including smoldering and chronic types, it might be a promising target for the development of a new anti-ATL therapy. The NOG mouse model system described in the present study could provide a novel means by which to understand and investigate the further importance of TSLC1 in ATL progression.

We thank S. Ichinose of the Instrumental Analysis Research Center; S. Endo of the Animal Research Center, Tokyo Medical and Dental University; and Y. Sato of the National Institute of Infectious Diseases for her excellent technical assistance. Anti-Tax (MI73) antibody was the kind gift of Y. Namba and M. Matsuoka (Institute for Virus Research, Kyoto University).

Supported by grants from the Ministry of Education, Science, and Culture; the Ministry of Health, Labor, and Welfare; and Human Health Science of Japan.

REFERENCES

1. **Ballard, D. W., E. Bohnlein, J. W. Lowenthal, Y. Wano, B. R. Franza, and W. C. Greene.** 1988. HTLV-I tax induces cellular proteins that activate the B element in the IL-2 receptor gene. Science **241**:1652–1655.
2. **Cross, S. L., M. B. Feinberg, J. B. Wolf, N. J. Holbrook, F. Wong-Staal, and W. J. Leonard.** 1987. Regulation of the human interleukin-2 receptor chain promoter: activation of a nonfunctional promoter by the transactivator gene of HTLV-I. Cell **49**:47–56.
3. **Dewan, M. Z., K. Terashima, M. Taruishi, H. Hasegawa, M. Ito, Y. Tanaka, N. Mori, T. Sata, Y. Koyanagi, M. Maeda, Y. Kubuki, A. Okayama, M. Fujii, and N. Yamamoto.** 2003. Rapid tumor formation of human T-cell leukemia virus type 1-infected cell lines in novel NOD-SCID/γ_c^{null} mice: suppression by an inhibitor against NF-κB. J. Virol. **77**:5286–5294.
4. **Dewan, M. Z., J. N. Uchihara, K. Terashima, M. Honda, T. Sata, M. Ito, N. Fujii, K. Uozumi, K. Tsukasaki, M. Tomonaga, Y. Kubuki, A. Okayama, M. Toi, N. Mori, and N. Yamamoto.** 2006. Efficient intervention of growth and infiltration of primary adult T-cell leukemia cells by an HIV protease inhibitor, ritonavir. Blood **107**:716–724.
5. **Felber, B. K., H. Paskalis, C. Kleinman-Ewing, F. Wong-Staal, and G. N. Pavlakis.** 1985. The pX protein of HTLV-I is a transcriptional activator of its long terminal repeats. Science **229**:675–679.
6. **Furuta, R. A., K. Sugiura, S. Kawakita, T. Inada, S. Ikehara, T. Matsuda, and J. Fujisawa.** 2002. Mouse model for the equilibration interaction between the host immune system and human T-cell leukemia virus type 1 gene expression. J. Virol. **76**:2703–2713.
7. **Hinuma, Y., K. Nagata, M. Hanaoka, M. Nakai, T. Matsumoto, K. I. Kinoshita, S. Shirakawa, and I. Miyoshi.** 1981. Adult T-cell leukemia: antigen in an ATL cell line and detection of antibodies to the antigen in human sera. Proc. Natl. Acad. Sci. USA **78**:6476–6480.
8. **Ito, M., H. Hiramatsu, K. Kobayashi, K. Suzue, M. Kawahata, K. Hioki, Y. Ueyama, Y. Koyanagi, K. Sugamura, K. Tsuji, T. Heike, and T. Nakahata.** 2002. NOD/SCID/γcnull mouse: an excellent recipient mouse model for engraftment of human cells. Blood **100**:3175–3182.
9. **Kuramochi, M., H. Fukuhara, T. Nobukuni, T. Kanbe, T. Maruyama, H. P. Ghosh, M. Pletcher, M. Isomura, M. Onizuka, T. Kitamura, T. Sekiya, R. H. Reeves, and Y. Murakami.** 2001. TSLC1 is a tumor suppressor gene in human non-small cell lung cancer. Nat. Genet. **27**:427–730.
10. **Maeda, M., A. Shimizu, K. Ikuta, H. Okamoto, M. Kashihara, T. Uchiyama, T. Honjo, and J. Yodoi.** 1985. Origin of human T-lymphotrophic virus I-positive T cell lines in adult T cell leukemia. Analysis of T cell receptor gene rearrangement. J. Exp. Med. **162**:2169–2174.
11. **Maruyama, M., H. Shibuya, H. Harada, M. Hatakeyama, M. Seiki, T. Fujita, J. Inoue, M. Yoshida, and T. Taniguchi.** 1987. Evidence for aberrant activation of the interleukin-2 autocrine loop by HTLV-1-encoded p40x and T3/Ti complex triggering. Cell **48**:343–350.
12. **Masuda, M., M. Yagita, H. Fukuhara, M. Kuramochi, T. Maruyama, A. Nomoto, and Y. Murakami.** 2002. The tumor suppressor protein TSLC1 is involved in cell-cell adhesion J. Biol. Chem. **277**:31014–31019.
13. **Murakami, Y., T. Nobukuni, K. Tamura, T. Maruyama, T. Sekiya, Y. Arai, H. Gomyou, A. Tanigami, M. Ohki, D. Cabin, P. Frischmeyer, P. Huni, and R. H. Reeves.** 1998. Localization of tumor suppressor activity important in non-small cell lung carcinoma on chromosome 11q. Proc. Natl. Acad. Sci. USA **95**:8153–8158.
14. **Poiesz, B. J., F. W. Ruscetti, A. F. Gazdar, P. A. Bunn, J. D. Minna, and R. C. Gallo.** 1980. Detection and isolation of type C retrovirus particles from fresh and cultured lymphocytes of a patient with cutaneous T-cell lymphoma. Proc. Natl. Acad. Sci. USA **77**:7415–7419.
15. **Sasaki, H., I. Nishikata, T. Shiraga, E. Akamatsu, T. Fukami, T. Hidaka, Y. Kubuki, A. Okayama, K. Hamada, H. Okabe, Y. Murakami, H. Tsubouchi, and K. Morishita.** 2005. Overexpression of a cell adhesion molecule, TSLC1, as a possible molecular marker for acute type of adult T-cell leukemia. Blood **105**:1204–1213.
16. **Sodroski, J. G., C. A. Rosen, and W. A. Haseltine.** 1984. Transacting transcriptional activation of the long terminal repeat of human T lymphotropic viruses in infected cells. Science **225**:381–385.
17. **Yamaguchi, K., and T. Watanabe.** 2002. Human T lymphotropic virus type-I and adult T-cell leukemia in Japan. Int. J. Hematol. **76**:240–245.
18. **Yoshida, M., I. Miyoshi, and Y. Hinuma.** 1982. Isolation and characterization of retrovirus from cell lines of human adult T-cell leukemia and its implication in the disease. Proc. Natl. Acad. Sci. USA **79**:2031–2035.

ELSEVIER

INSTITUT PASTEUR

Microbes and Infection 10 (2008) 748–756

www.elsevier.com/locate/micinf

Original article

Induction of apoptosis in Epstein-Barr virus-infected B-lymphocytes by the NF-κB inhibitor DHMEQ

Ariko Miyake [a,1], Md. Zahidunnabi Dewan [b,c,1], Takaomi Ishida [a], Mariko Watanabe [d], Mitsuo Honda [c], Tetsutaro Sata [e], Naoki Yamamoto [b,c,**], Kazuo Umezawa [f], Toshiki Watanabe [a,***], Ryouichi Horie [d,*]

[a] *Laboratory of Tumor Cell Biology, Department of Medical Genome Sciences, Graduate School of Frontier Sciences, University of Tokyo, 4-6-1 Shirokanedai, Minato-ku, Tokyo 108-8639, Japan*

[b] *Department of Molecular Virology, Bio-Response, Graduate School, Tokyo Medical and Dental University, 1-5-45 Yushima, Bunkyo-ku, Tokyo 113-8519, Japan*

[c] *AIDS Research Center, National Institute of Infectious Diseases, 1-23-1 Toyama, Shinjuku-ku, Tokyo 162-8640, Japan*

[d] *Department of Hematology, School of Medicine, Kitasato University, 1-15-1 Sagamihara, Kanagawa 228-8555, Japan*

[e] *Department of Pathology, National Institute of Infectious Diseases, 1-23-1 Toyama, Shinjuku-ku, Tokyo 162-8640, Japan*

[f] *Department of Applied Chemistry, Faculty of Science and Technology, Keio University, 3-14-1 Hiyoshi, Kohoku-ku, Yokohama, Kanagawa 223-0061, Japan*

Received 19 January 2008; accepted 9 April 2008
Available online 13 April 2008

Abstract

Epstein–Barr virus (EBV) causes EBV-associated lymphoproliferative diseases in patients with profound immune suppression. Most of these diseases are life-threatening and the prognosis of AIDS-associated lymphomas is extremely unfavorable. Polyclonal expansion of virus infected B-cell predisposes them to transformation. We investigated the possibility of nuclear factor kappa B (NF-κB) inhibition by dehydroxymethylepoxyquinomicin (DHMEQ) for the treatment and prevention of EBV-associated lymphoproliferative diseases. We examined the effect of DHMEQ on apoptosis induction in four EBV-transformed lymphoblastoid cell lines as well as peripheral blood mononuclear cells infected with EBV under immunosuppressed condition. DHMEQ inhibits NF-κB activation in EBV-transformed lymphoblastoid cell lines and induces apoptosis by activation of mitochondrial and membranous pathways. Using an *in vivo* NOD/SCIDγc mouse model, we showed that DHMEQ has a potent inhibitory effect on the growth of lymphoblastoid cells. In addition, DHMEQ selectively purges EBV-infected cells expressing latent membrane protein (LMP) 1 from peripheral blood mononuclear cells and inhibits the outgrowth of lymphoblastoid cells. These results suggest that NF-κB is a molecular target for the treatment and prevention of EBV-associated lymphoproliferative diseases. As a potent NF-κB inhibitor, DHMEQ is a potential compound for applying this strategy in clinical medicine.

Keywords: Epstein–Barr virus infections; NF-κB; DHMEQ

1. Introduction

Epstein–Barr virus (EBV) is a member of the γ-herpesvirus family that infects more than 90% of the world population and initially establishes latency III infection in B lymphocytes [1]. Latency III infection is characterized by the expression of the entire array of EBV latency genes, including EBV nuclear proteins (EBNA1, -2, -3A, -3B, -3C, and -LP), integral latent membrane proteins (LMP1, -2A, and -2B), the BamA

* Corresponding author. Tel.: +81 42 778 8111; fax: +81 42 778 8441.
** Tel.: +81 3 5803 5178; fax: +81 3 5803 0124.
*** Tel.: +81 3 5449 5298; fax: +81 3 5449 5418.
E-mail addresses: yamamoto.mmb@tmd.ac.jp (N. Yamamoto), tnabe@ims.u-tokyo.ac.jp (T. Watanabe), rhorie@med.kitasato-u.ac.jp (R. Horie).
[1] These authors contributed equally to this work.

1286-4579/$ - see front matter © 2008 Elsevier Masson SAS. All rights reserved.
doi:10.1016/j.micinf.2008.04.002

rightward transcripts (BARTs), and small RNAs (EBERs). Immune response mediated by T-lymphocytes eliminates most latency III-infected cells; however, resting memory B lymphocytes provide a reservoir for latent virus. T-lymphocyte immunity to latency III-infected B lymphocytes persists for life and protects reactivation of latent virus from a reservoir [2].

However, in the absence of an effective immune response, reactivation of latent virus from a reservoir occurs and causes EBV-associated lymphoproliferative diseases. EBV-associated lymphoproliferative diseases occur with primary infection after transplantation or reactivation of latent virus as a consequence of immune suppression for organ transplantation and autoimmune diseases or acquired immune deficiency syndrome (AIDS) [3–6]. EBV-associated lymphoproliferative diseases are associated in the majority of cases with latency type III phenotype. The prognosis of EBV-associated lymphoproliferative diseases is variable; however, most of these are life-threatening and the prognosis of AIDS-associated lymphomas is extremely unfavorable, although introduction of highly active anti-retroviral treatment (HAART) decreased the incidence, increased the effectiveness of chemotherapy, and improved survival [5]. EBV infection of B-lymphocytes *in vitro* also results in latency III infection and sustained cell proliferation as lymphoblastoid cell lines (LCLs).

Activation of nuclear factor kappa B (NF-κB) has been connected with resistance against apoptosis and tumorigenesis [7]. Despite the diversity in clinical manifestations of EBV-associated lymphoproliferative diseases, strong and constitutive NF-κB activity is reported to be a common characteristic of this disease entity. LMP1 mimics signaling from tumor necrosis factor (TNF) receptor family members by association with tumor necrosis factor receptor-associated factors (TRAFs) and activates the IKK (IκB kinase)−NF-κB pathway [8].

NF-κB represents five cellular proteins: c-Rel, RelA (p65), RelB, NF-κB1 (p50 and its precursor p105), and NF-κB2 (p52 and its precursor p100). The IκB inhibitory proteins consist of IκBα, IκBβ, IκBε, IκBγ, and Bcl-3. NF-κB forms homo- or heterodimers and exists as an inactive complex with IκB regulatory proteins in the cytoplasm. Various signaling pathways converge into IKK-mediated degradation of IκB proteins and subsequent release of uncomplexed NF-κB, which then migrates into the nucleus and activates the transcription of target genes [9].

Dehydroxymethylepoxyquinomicin (DHMEQ) is a new NF-κB inhibitor that is a 5-dehydroxymethyl derivative of the novel compound epoxyquinomicin C that has a 4-hydroxy-5,6-epoxycyclohexenone structure like panepoxydone. Panepoxydone had been found to inhibit TNF-α-induced activation of NF-κB [10]. We have shown that DHMEQ inhibits NF-κB at the level of nuclear translocation [11].

In this study, to investigate the possibility of NF-κB inhibition by DHMEQ as a strategy for the treatment and prevention of EBV-associated lymphoproliferative diseases, we investigated the effect of DHMEQ on apoptosis induction in four EBV-transformed LCLs as well as peripheral blood mononuclear cells (PBMC) in the early phase of EBV infection, and further examined the molecular mechanism of DHMEQ-induced apoptosis.

2. Materials and methods

2.1. Cells

B95.8 EBV-transformed LCLs were established by infection of lymphocytes from four healthy donors with culture supernatants of the virus producer B95.8 line as described previously [12], and are indicated in the text by the first two letters of the name of each donor. In all experiments to test the effects of DHMEQ treatment, LCLs were maintained in RPMI 1640 medium supplemented with 10% fetal bovine serum (FBS).

2.2. Chemicals

DHMEQ is an NF-κB inhibitor that blocks nuclear translocation of NF-κB [11]. DHMEQ was dissolved with dimethylsulfoxide (DMSO). DHMEQ or DMSO was used for experiments at indicated concentrations. Bisbenzimide H 33342 fluorochrome (Hoechst 33342) was purchased from Calbiochem (Bad Soden, Germany).

2.3. Electrophoretic mobility shift analysis

Electrophoretic mobility shift analysis (EMSA) was carried out according to the methods described previously [13]. For detecting NF-κB binding, a double-stranded oligonucleotide containing the κB site of the promoter for the mouse H-2Kb class I major histocompatibility antigen gene was used as a probe [14]. The nucleotide sequence is 5′-GAT CCG GCT GGG AAT CCC CGC TGG GAA TCC CCA TCT A-3′. For control EMSA, a double-strand oligonucleotide containing Oct-1 consensus sequence (Promega, Madison, WI, USA) was used as a probe. Antibodies used for supershift assays were as follows: NF-κB p50 (C-19) goat polyclonal antibody, rabbit polyclonal antibody for NF-κB p65 (C-20) and RelB (C-19), and mouse monoclonal antibody for c-Rel (B-6) and NF-κB p52 (C-5) (all from Santa Cruz Biotechnology Inc., Santa Cruz, CA). A mouse IgG antibody (Sigma, St. Louis, MO) served as a control.

2.4. Cell viability assay

The effects of DHMEQ on cell viability were assayed by color reaction with a tetrazolium salt, WST-8(4-[3-(2-methoxy-4-nitrophenyl)-2-[4-nitrophenyl]-2*H*-5-tetrazolio]-1,3-benzene disulfonate sodium salt) (Cell Counting Kit-8; Dojindo Laboratories, Kumamoto, Japan). After incubation with DHMEQ or DMSO at the indicated concentrations and time points, cells were treated with Cell Counting Kit-8 according to the manufacturer's recommendations and the results were measured by a microplate reader (Bio-Rad, Richmond, CA) at a test wavelength of 450 nm and reference wavelength of 630 nm.

2.5. Analysis of apoptosis and caspase activities

To quantify apoptosis, cells were labeled with fluorescein isothiocyanate (FITC)-conjugated Annexin V (BD Biosciences, Palo Alto, CA), then subjected to flow cytometric analysis. For analysis of nuclear DNA fragmentation, the terminal deoxynucleotidyl transferase (TdT)-mediated dUTP nick end-labeling (TUNEL) assay was done according to the manufacturer's recommendations (DeadEnd Fluorometric TUNEL Systems; Promega). Cells were analyzed using a FACS Calibur flow cytometer (BD Biociences) and fluorescence microscopy. Activities of caspase-3, -8, and -9 were determined by using green fluorochrome-labeled inhibitors of caspases (FLICA)-3, -8, and -9 (FLICA Apoptosis Detection Kit; Immunochemistry Technologies, Bloomington, MN). Cells from LCLs were treated with 10 μg/ml of DHMEQ (+) or with DMSO alone (−) for 8 h and fixed on slides; active caspases were detected by FLICA-3, -8, and -9. For detection of nuclear DNA, cells were stained with Hoechst 33342 and photographed through a UV filter and an Olympus BX50F microscope (Olympus, Tokyo, Japan).

2.6. In vivo effects of DHMEQ on NOG mice inoculated with LCLs

NOG mice were purchased from the Central Institute for Experimental Animals (Kawasaki, Japan). The Ethical Review

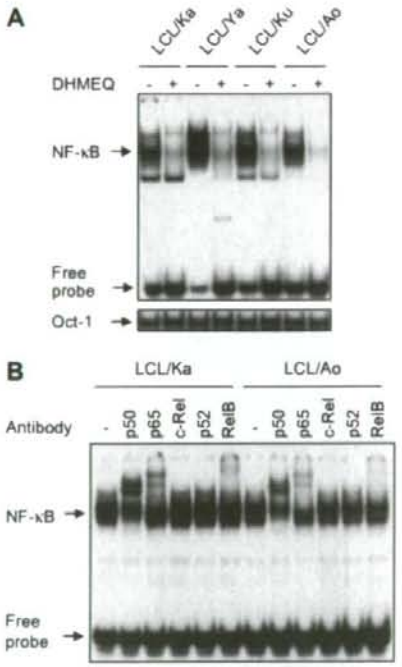

Fig. 1. Inhibition of constitutive NF-κB binding activity in LCLs by DHMEQ. (A) Inhibition of constitutive NF-κB activity in LCLs. LCLs were treated with 10 μg/ml of DHMEQ (+) or with DMSO alone (−) for 3 h. Nuclear extracts (2.5 μg) were examined for NF-κB binding activity by electrophoretic mobility shift analysis (EMSA) with a radiolabeled NF-κB-specific probe. Binding of Oct-1 served as a control. (B) Subcomponents of constitutive NF-κB activity in LCLs. Nuclear extracts (1 μg) of cells without DHMEQ treatment were subjected to supershift analysis with antibodies specific for NF-κB p50, p65, c-Rel, p52, and RelB or without antibody (−). The experiment using isotype matched IgG control showed the same result (data not shown). The position of shifted bands corresponding to NF-κB and free probes are indicated on the left.

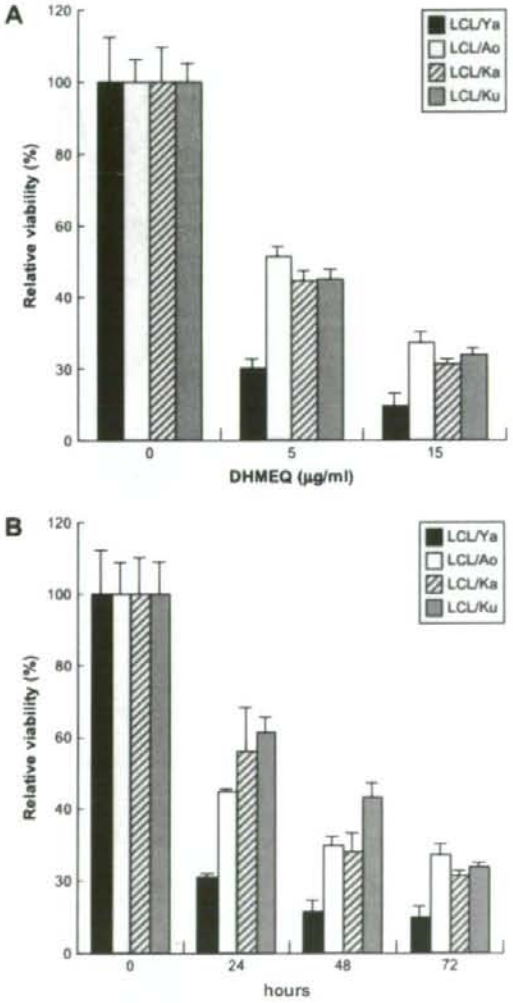

Fig. 2. DHMEQ inhibits proliferation of LCLs. The viability of the cells was determined by WST-8 assay and the relative levels compared with those of DMSO-treated cells are presented. Data represent the mean and standard deviation of triplicate experiments. (A) Results of dose–response experiments. LCLs were treated with 0, 5, or 10 μg/ml of DHMEQ for 72 h. ALL LCLs treated with 0, 5, or 10 μg/ml of DHMEQ showed statistical significance compared to DMSO-treated controls. (B) Results of time–response experiments. LCLs were treated with 10 μg/ml of DHMEQ for 24, 48, and 72 h. ALL LCLs treated for 24, 48, and 72 h except for LCL/Ku at the point of 24 h showed statistical significance compared to DMSO-treated controls.

Committee of the National Institute of Infectious Diseases approved the experimental protocol. 1×10^6 LCL cells were inoculated subcutaneously into the post-auricular region of NOG mice. DHMEQ was administered three times a week for 1 month into the post-auricular region of mice at a dose of 12 mg/kg, beginning on day 5 when tumors were palpable. The control mice were injected RPMI-1640 as was performed in our recent published papers [15,16]. Mice were killed 1 month after inoculation.

2.7. Immunohistochemistry

Cells were immunostained with antibodies and fluorescence signals were detected using confocal microscopy. Cytospin samples were prepared using 5×10^5 cells and cells were first washed three times with phosphate-buffered saline (PBS). Cells were then fixed with 100% cold acetone for 10 min at room temperature and washed three times in PBS. Samples were incubated with primary antibody at the concentration

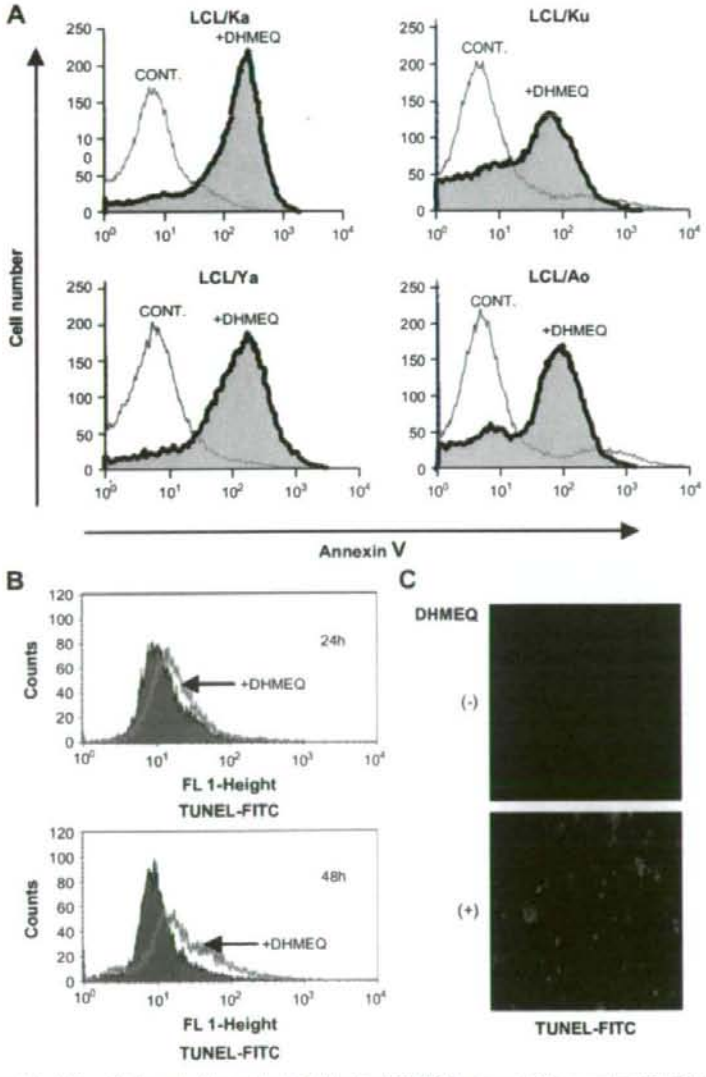

Fig. 3. DHMEQ induces apoptosis in LCLs. (A) Annexin V reactivity in LCLs after DHMEQ treatment. LCLs were treated with (filled curve) or without (open curve) 10 μg/ml of DHMEQ for 48 h, and the binding of FITC-conjugated Annexin V was analyzed by flow cytometry. (B) DNA fragmentation in LCL cells after DHMEQ treatment. DNA fragmentation in LCL cells was detected by TUNEL assay with flow cytometry. Representative flow cytometric profiles are shown for cells treated with 10 μg/ml of DHMEQ (open curve) or with DMSO alone (filled curve) for 24 h (upper panel) or 48 h (lower panel). (C) LCL cells were treated with 10 μg/ml of DHMEQ (+) or with DMSO alone (−) for 48 h, fixed on slides, and processed for TUNEL assay. A filter that selectively detects fluorescein isothiocyanate (FITC)-TUNEL fluorescence was used for the microscopic observation.

of 5 μg/ml at 4 °C overnight and washed with PBS three times. After incubation with fluorescence-labeled secondary antibody for 30 min at 37 °C, samples were washed three times in PBS and covered with a Perma Fluoro antifade reagent (Therme Shandon Co., Pittsburgh, PA). Fluorescence signals were detected using confocal microscopy (Radiance 2000) (Bio-Rad Laboratories. Antibodies used were as follows: anti-Epstein–Barr virus LMP clones CS, 1-4 mouse monoclonal antibody (Dako, Kyoto, Japan), and anti-p65 (c-20) goat polyclonal antibody (Santa Cruz Biotechnology Inc.

2.8. Real-time quantitative PCR

The expression level of anti-apoptotic genes was quantified by real-time reverse transcription–polymerase chain reaction (RT–PCR). Total RNA was extracted from the cells by ISOGEN reagent (Nippon Gene Co., Toyama, Japan) and treated according to the manufacturer's instructions. cDNA was synthesized using oligo dT and random primers synthesized with a PrimeScript RT reagent kit (Takara Bio Inc., Shiga, Japan). Amplification was performed with SYBR premix Ex Taq (Takara Bio Inc.) and the primer sets for c-IAP1, Bfl-1, BCL-XL, and c-FLIP (Takara Bio Inc.). The viral DNA load in EBV-infected PBMC was determined by real-time PCR with slight modifications of a previously described method [17]. DNA samples were extracted from the cells with a DNeasy tissue kit (Qiagen, Hilden, Germany). Amplification with SYBR premix Ex Taq (Takara Bio Inc.) and primers for BALF5 gene encoding the viral DNA polymerase (5′-CGG AAG CCC TCT GGA CTT C-3′ and 5′-CCC TGT TTA TCC GAT GGA ATG-3′) was performed using the Thermal Cycler Dice Real Time System (Takara Bio Inc.) and analyzed using the manufacturer's software.

2.9. Statistical analysis

Differences between mean values were assessed by *t*-test. A *P*-value of <0.05 was considered to be statistically significant.

3. Results

3.1. DHMEQ efficiently blocks constitutive NF-κB activity in LCLs

We first examined the effects of DHMEQ against constitutive NF-κB activity in established LCLs. Treatment with DHMEQ at a concentration of 10 μg/ml abrogated constitutive NF-κB binding activity in these cell lines (Fig. 1A). Components of NF-κB that are constitutively activated in LCLs were analyzed by

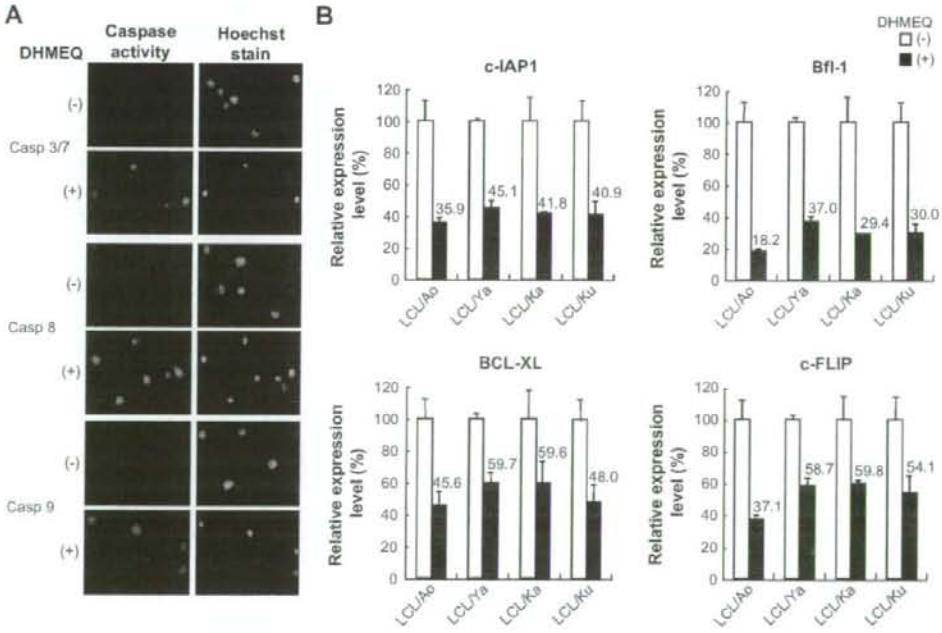

Fig. 4. Activation of caspase-3, -8, and -9. (A) LCL cells were treated with 10 μg/ml of DHMEQ (+) or with DMSO alone (−) for 8 h and fixed on slides. Caspase-3/7, -8, and -9 activities in LCLs after DHMEQ treatment were detected by green fluorochrome-labeled inhibitors of caspases (FLICA)-3/7, -8, and -9 (left panels) and nuclear DNA was stained with Hoechst 33342 (right panels). (B) Effects of DHMEQ on genes regulating apoptosis in LCLs. Quantification of the gene expression by real-time PCR. LCLs were treated with 10 μg/ml of DHMEQ (+) or with DMSO alone (−) for 4 h. The expressions of c-IAP1, Bfl-1, BCL-XL, and c-FLIP were quantified by real-time PCR. The data are means with standard deviation of triplicate experiments. The numbers above the bar graphs indicate the means of each gene expression after DHMEQ treatment. The reduction of the expressions of c-IAP1, Bfl-1, BCL-XL, and c-FLIP was statistically significant.

supershift assays. The results revealed that the NF-κB components consist of p50, p65, and RelB (Fig. 1B).

3.2. DHMEQ induces apoptosis of LCLs

To study the significance of NF-κB activation in the growth of LCLs, we examined the effects of DHMEQ on cell viability. Results of WST-8 assays showed that DHMEQ treatment reduced the cell viability of all four LCLs in a dose- and time-dependent manner (Fig. 2A and B).

NF-κB plays a key role in resistance to apoptosis [18]. Thus, we next examined whether DHMEQ induces apoptosis of LCLs by analyzing Annexin V reactivity and DNA fragmentation. Flow cytometric analysis showed a significant increase in the number of Annexin V-positive cells after DHMEQ treatment (Fig. 3A). Fragmentation of the nuclei of LCLs was clearly demonstrated after DHMEQ treatment by the TUNEL assay (Fig. 3B and C).

3.3. DHMEQ-induced apoptosis involves activation of caspases 3, 8, and 9

To confirm that the induction of apoptosis in LCLs by DHMEQ is caused by activation of the caspase pathway, we first examined activation of caspase-3/7 by immunostaining, using an antibody that recognizes a cleaved form of caspase-3/7. Results clearly showed cleavage of caspase-3/7, confirming that DHMEQ-induced apoptosis is associated with activation of the caspase pathway (Fig. 4A, top). To differentiate the membranous and mitochondrial pathways, we next examined the activation of caspases 8 and 9, which are upstream of caspase-3/7, by immunostaining. DHMEQ-treated LCL cells showed activation of both caspase-8 and caspase-9 (Fig. 4A, middle and bottom).

To understand the molecular mechanisms of apoptosis induction of LCLs after NF-κB inhibition by DHMEQ, we next examined by quantitative RT–PCR the changes in the expression levels of anti-apoptotic genes c-IAP1, Bfl-1, Bcl-XL, and c-FLIP, reportedly under the control of NF-κB, after DHMEQ treatment. The results demonstrated down-regulation of all of these genes (Fig. 4B).

3.4. DHMEQ shows a potent inhibitory effect on the growth of LCL cells in NOG mice

Because results *in vitro* suggested potential efficacy of DHMEQ for the treatment of patients with EBV-associated lymphoproliferative diseases, we next examined whether DHMEQ treatment can suppress the growth of xenografted LCL cells in a NOG mouse model. The gross appearance of resected tumors in mice treated with DHMEQ showed reduction of the tumor mass 1 month after inoculation of LCL cells (Fig. 5A and B). A decrease in the size of tumors in mice treated with DHMEQ was demonstrated when compared with controls 1 month after the injection of LCL cells (Fig. 5C).

3.5. DHMEQ inhibits outgrowth of EBV-infected peripheral blood B-lymphocytes

EBV-infected B lymphocytes under immunocompromised conditions acquire latency III infection, which may lead to proliferation and transformation into lymphoproliferative diseases including lymphomas [2,3]. Previous data link NF-κB activation by LMP-1 to transformation; however, they also indicate that NF-κB activation is not sufficient for transformation and should coordinate with other signals like mitogen-activated protein kinases [19]. Roles of NF-κB activity in EBV-infected lymphocytes for their survival during the early phase of infection are not fully understood. Therefore, to investigate the roles of NF-κB activation on the survival of EBV-infected lymphocytes during the early phase of infection, we examined the effect of NF-κB inhibition by DHMEQ on their survival and the EBV viral load in PBMC infected with EBV. Lymphocytes infected with EBV under immunosuppressive conditions already show constitutive NF-κB activation as well as LMP1 expression. Treatment of these cells with DHMEQ inhibited translocation of NF-κB into the nucleus (Fig. 6A). DHMEQ treatment also eliminated LMP1-expressing lymphocytes from PBMC (Fig. 6B). Finally, DHMEQ treatment prevented the outgrowth of lymphocytes infected

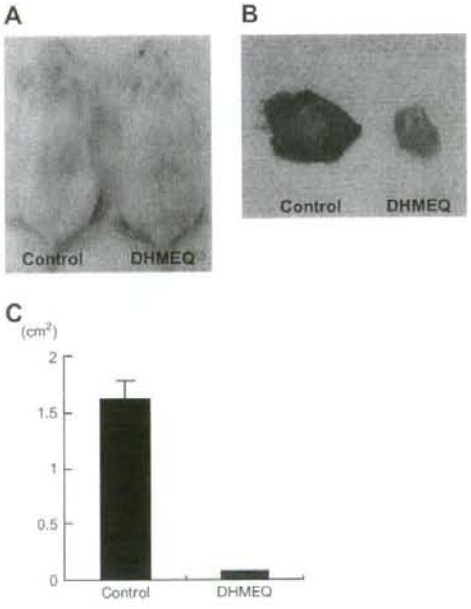

Fig. 5. DHMEQ inhibited the tumor growth of LCL cells *in vivo*. NOG mice were inoculated with LCL cells and administered DHMEQ (12 mg/kg) ($n = 5$) or control medium ($n = 5$) subcutaneously in the post-auricular region three times a week for up to 1 month. (A) Photograph of the backs of mice. (B) Photograph of a tumor at the site of LCL cells inoculation. (C) Subcutaneous tumor volume of mice inoculated with LCL cells and administered DHMEQ or control medium 1 month after inoculation.

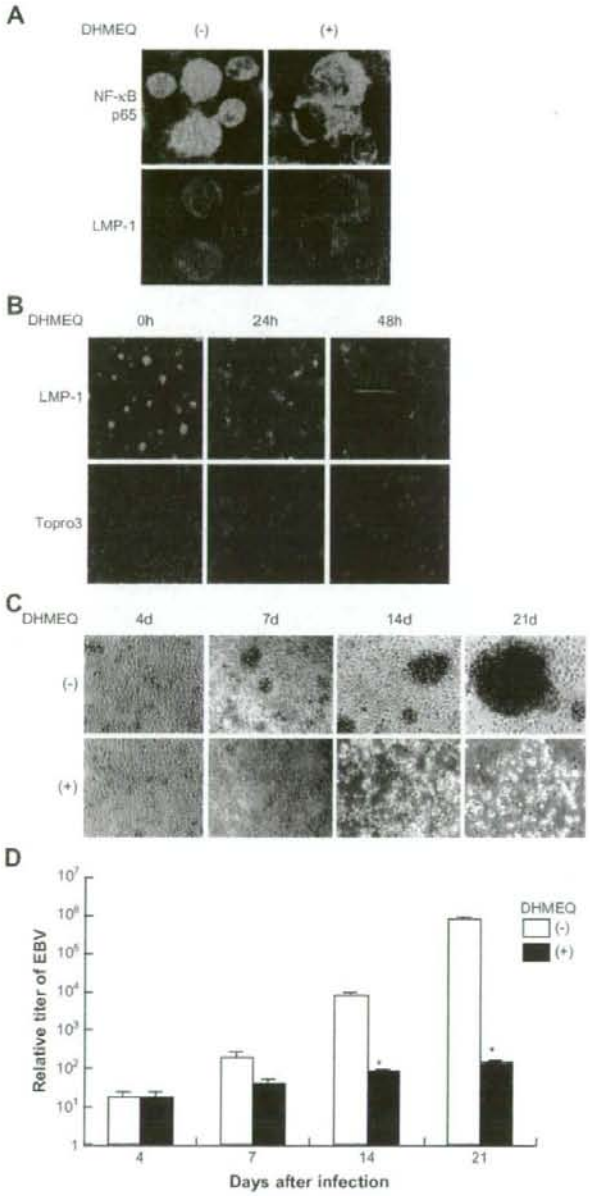

Fig. 6. Effects of DHMEQ on PBMC infected with EBV. 8×10^5/ml of PBMC from a healthy donor infected with EBV using supernatant of B95.8 line were cultured in RPMI 1640 medium supplemented with 10% FBS and 200 ng/ml cyclosporine A. Cells were harvested 4 days and 14 days after infection and served for experiments. (A) Inhibition of NF-κB and expression of LMP1 in lymphocytes. At the point of 4 days after infection, cells were treated with or without 10 μg/ml of DHMEQ for 1 h and immunostained with antibodies for LMP1 and NF-κB p65. DMSO-treated cells served as a control. (B) DHMEQ treatment eliminated LMP1 expressing cells from PBMC. At the point of 14 days after infection, cells were treated with or without 10 μg/ml DHMEQ for the indicated number of hours. Cells stained with anti-LMP1 antibody and topro 3 were observed by confocal microscopy. DMSO-treated cells served as a control. (C, D) Photographs of EBV-infected PBMC and quantification of viral load by real-time PCR. Cells cultured for 4 days were treated with 10 μg/ml of DHMEQ (+) or with DMSO alone (−) thereafter twice a week. Cells were observed by microscopy at the indicated days (C). Cells were harvested on the indicated days and genomic DNA was isolated. The viral load was quantified by real-time PCR as described in Section 2. The data are means and standard deviations of triplicate experiments (D). The asterisks indicate statistical significance.

with EBV and decreased the EBV viral load in PBMC (Fig. 6C and D).

4. Discussion

In the present study, we showed that the NF-κB inhibitor DHMEQ blocked strong and constitutive NF-κB activity, reduced viability, and induced apoptosis in LCLs. Induction of apoptosis by DHMEQ in LCLs is associated with inhibition of NF-κB, which is followed by down-regulation of NF-κB regulated anti-apoptotic genes. These observations, combined with our previous study about the mechanisms of action of DHMEQ [11], indicate that apoptosis induction of LCLs by DHMEQ is mediated by inhibitory effect of DHMEQ against NF-κB. DHMEQ appears to be more specific to NF-κB pathway compared with IκB kinase (IKK) inhibitor, Bay 11-7082 used in the previous studies [20,21], because DHMEQ inhibits downstream of IKK and Bay 11-7082 has been reported to be apparently not specific for NF-κB pathway [22]. Therefore our study provides further evidence for the importance of NF-κB in the survival of LCLs and indicates effectiveness of DHMEQ in the treatment of EBV-infected transformed lymphocytes.

We also showed that DHMEQ inhibits constitutive NF-κB activation in B lymphocytes expressing LMP1, eliminates these cells from PBMC, and inhibits the outgrowth of lymphoblastic cells. The results indicate that B lymphocytes become dependent on NF-κB for proliferation and survival within several days after EBV infection. Although previous data indicate that not only NF-κB but also other signals like mitogen-activated protein kinases are involved in transformation of lymphocytes to LCL cells [19], the results in this study indicates that abrogation of constitutive NF-κB activity appears to be sufficient to prevent transformation of EBV-infected lymphocytes. Previous reports underscored constitutive NF-κB activity as a molecular target in LCL cells [20,21,23]. Our study shows a new insight that constitutive NF-κB activity is a common molecular target in EBV-infected transformed and untransformed lymphocytes.

Recent reports showed that EBV viral load is a useful marker for disease status of lymphoproliferative diseases or lymphomas in patients with immunosuppression [24]. We showed that DHMEQ treatment prevented the increase of EBV viral load in PBMC. The reduction of EBV viral load in PBMC by DHMEQ indicates not only that the elimination of lymphocytes infected by EBV contributes to the reduction, but also that the replication of EBV virus may depend on NF-κB activity. However, previous studies showed that NF-κB activity does not promote replication of EBV virus, but rather inhibits its replication [25]. Therefore, reduction of viral load in lymphocytes infected with EBV treated with DHMEQ appears to be due to the elimination of lymphocytes infected with EBV. Collectively, early detection of the increase of EBV viral load and purging infected cells under transformation by a NF-κB inhibitor may contribute to the preventive intervention against lymphoproliferative diseases in patients with profound immunosuppression.

Our results suggest that the effects of DHMEQ depend on the down-regulation of NF-κB-dependent genes that control apoptosis. Down-regulation of c-FLIP, involved in anti-apoptosis blocking caspase-8, as well as Bfl-1, Bcl-XL and c-IAP, involved in the anti-apoptosis blocking caspase-9, by DHMEQ may result in activation of membranous and mitochondrial pathways, respectively [26]. This implies the possibility that in EBV-infected lymphocytes, the induction of anti-apoptotic genes is counteracting the apoptotic pressure and preventing these cells from undergoing apoptosis.

The mice treated with DHMEQ in 1% DMSO did not show any relevant signs of toxicity such as body weight loss in this experiment. The dose of DHMEQ administered in this experiment was 12 mg/kg three times a week, far less than the LD_{50} of DHMEQ, 180 mg/kg (Naoki Matsumoto, K.U., unpublished observation, July 1999). Results of our in vivo model suggest that DHMEQ may be feasible and less toxic at an effective dose, although the pharmacokinetics has not yet been elucidated. In our NOG mice model, the results indicate that local administration of DHMEQ can prevent primary tumor growth without significant signs of toxicity. Additional experiments, which include intraperitoneal and intravenous administration of DHMEQ, will further confirm efficacy of DHMEQ against LCLs *in vivo*.

Our recent study also indicates that DHMEQ has little effect on the viability of PBMC or purified B cells *in vitro* under almost the same experimental condition as this study [27]. These *in vitro* and *in vivo* results suggest a favorable toxic profile and potent NF-κB inhibitory effect by DHMEQ. Thus, DHMEQ appears to be a candidate for the treatment of EBV-associated lymphoproliferative diseases as well as for their chemoprevention.

In conclusion, our study indicates that the unique NF-κB inhibitor DHMEQ is a potential compound that targets constitutive activation of NF-κB in EBV-infected transformed and untransformed B cells. Because EBV-associated lymphoproliferative diseases are life-threatening and the prognosis of AIDS-associated lymphomas is extremely unfavorable, our results support preventive intervention with a NF-κB inhibitor as a new strategy in patients with immunosuppression.

Acknowledgments

This work was supported in part by Grants-in-Aid for Scientific Research from the Japan Society for Promotion of Science (R.H. and T.W.). This work was also supported by grants from the Japanese Ministries of Education, Culture, Sport Science and Technology and Health, Labour and Welfare, as well as the Human Health Science of Japan (N.Y.).

References

[1] J.I. Cohen, Epstein–Barr virus infection, N. Engl. J. Med 343 (2000) 481–492.
[2] K.F. Macsween, D.H. Crawford, Epstein–Barr virus-recent advances, Lancet Infect. Dis 3 (2003) 131–140.
[3] E. Klein, L.L. Kis, G. Klein, Epstein–Barr virus infection in humans: from harmless to life endangering virus-lymphocyte interactions, Oncogene 26 (2007) 1297–1305.

[4] S. Gottschalk, C.M. Rooney, H.E. Heslop, Post-transplant lymphoproliferative disorders, Annu. Rev. Med 56 (2005) 29–44.
[5] C. Diamond, T.H. Taylor, T. Aboumrad, H. Anton-Culver, Changes in acquired immunodeficiency syndrome-related non-Hodgkin lymphoma in the era of highly active antiretroviral therapy: incidence, presentation, treatment, and survival, Cancer 106 (2006) 128–135.
[6] Y. Hoshida, J.X. Xu, S. Fujita, I. Nakamichi, J. Ikeda, Y. Tomita, S. Nakatsuka, J. Tamaru, A. Iizuka, T. Takeuchi, K. Aozasa, Lymphoproliferative disorders in rheumatoid arthritis: clinicopathological analysis of 76 cases in relation to methotrexate medication, J. Rheumatol 34 (2007) 322–331.
[7] D.C. Guttridge, C. Albanese, J.Y. Reuther, R.G. Pestell, A.S. Baldwin Jr., NF-kappaB controls cell growth and differentiation through transcriptional regulation of cyclin D1, Mol. Cell. Biol. 19 (1999) 5785–5799.
[8] O. Devergne, E. Hatzivassiliou, K.M. Izumi, K.M. Kaye, M.F. Kleijnen, E. Kieff, G. Mosialos, Association of TRAF1, TRAF2, and TRAF3 with an Epstein–Barr virus LMP1 domain important for B-lymphocyte transformation: role in NF-kappaB activation, Mol. Cell. Biol. 16 (1996) 7098–7108.
[9] T.D. Gilmore, Introduction to NF-kappaB: players, pathways, perspectives, Oncogene 25 (2006) 6680–6684.
[10] N. Matsumoto, A. Ariga, S. To-e, H. Nakamura, N. Agata, S. Hirano, J. Inoue, K. Umezawa, Synthesis of NF-kappaB activation inhibitors derived from epoxyquinomicin C, Bioorg. Med. Chem. Lett. 10 (2000) 865–869.
[11] A. Ariga, J. Namekawa, N. Matsumoto, J. Inoue, K. Umezawa, Inhibition of tumor necrosis factor-alpha-induced nuclear translocation and activation of NF-kappa B by dehydroxymethylepoxyquinomicin, J. Biol. Chem. 277 (2002) 24625–24630.
[12] G. Miller, M. Lipman, Comparison of the yield of infectious virus from clones of human and simian lymphoblastoid lines transformed by Epstein–Barr virus, J. Exp. Med 138 (1973) 1398–1412.
[13] N.C. Andrews, D.V. Faller, A rapid micropreparation technique for extraction of DNA-binding proteins from limiting numbers of mammalian cells, Nucleic Acids Res. 19 (1991) 2499.
[14] J. Inoue, L.D. Kerr, L.J. Ransone, E. Bengal, T. Hunter, I.M. Verma, c-rel activates but v-rel suppresses transcription from kappa B sites, Proc. Natl. Acad. Sci. USA 88 (1991) 3715–3719.
[15] M.Z. Dewan, J.N. Uchihara, K. Terashima, M. Honda, T. Sata, M. Ito, N. Fujii, K. Uozumi, K. Tsukasaki, M. Tomonaga, Y. Kubuki, A. Okayama, M. Toi, N. Mori, N. Yamamoto, Efficient intervention of growth and infiltration of primary adult T-cell leukemia cells by an HIV protease inhibitor, ritonavir, Blood 107 (2006) 716–724.
[16] M. Watanabe, M.Z. Dewan, T. Okamura, M. Sasaki, K. Itoh, M. Higashihara, H. Mizoguchi, M. Honda, T. Sata, T. Watanabe, N. Yamamoto, K. Umezawa, R. Horie, A novel NF-kappaB inhibitor DHMEQ selectively targets constitutive NF-kappaB activity and induces apoptosis of multiple myeloma cells in vitro and in vivo, Int. J. Cancer 114 (2005) 32–38.
[17] H. Kimura, M. Morita, Y. Yabuta, K. Kuzushima, K. Kato, S. Kojima, T. Matsuyama, T. Morishima, Quantitative analysis of Epstein–Barr virus load by using a real-time PCR assay, J. Clin. Microbiol. 37 (1999) 132–136.
[18] J. Dutta, Y. Fan, N. Gupta, G. Fan, C. Gelinas, Current insights into the regulation of programmed cell death by NF-kappaB, Oncogene 25 (2006) 6800–6816.
[19] E.D. Cahir McFarland, K.M. Izumi, G. Mosialos, Epstein–Barr virus transformation: involvement of latent membrane protein 1-mediated activation of NF-kappaB, Oncogene 18 (1999) 6959–6964.
[20] E.D. Cahir-McFarland, K. Carter, A. Rosenwald, J.M. Giltnane, S.E. Henrickson, L.M. Staudt, E. Kieff, Role of NF-kappa B in cell survival and transcription of latent membrane protein 1-expressing or Epstein–Barr virus latency III-infected cells, J. Virol 78 (2004) 4108–4119.
[21] S.A. Keller, D. Hernandez-Hopkins, J. Vider, V. Ponomarev, E. Hyjek, E.J. Schattner, E. Cesarman, NF-kappaB is essential for the progression of KSHV- and EBV-infected lymphomas in vivo, Blood 107 (2006) 3295–3302.
[22] J.W. Pierce, R. Schoenleber, G. Jesmok, J. Best, S.A. Moore, T. Collins, M.E. Gerritsen, Novel inhibitors of cytokine-induced IkappaBalpha phosphorylation and endothelial cell adhesion molecule expression show anti-inflammatory effects in vivo, J. Biol. Chem. 272 (1997) 21096–21103.
[23] E.D. Cahir-McFarland, D.M. Davidson, S.L. Schauer, J. Duong, E. Kieff, NF-kappa B inhibition causes spontaneous apoptosis in Epstein–Barr virus-transformed lymphoblastoid cells, Proc. Natl. Acad. Sci. USA 97 (2000) 6055–6060.
[24] S.M. Aalto, E. Juvonen, J. Tarkkanen, L. Volin, T. Ruutu, P.S. Mattila, H. Piiparinen, S. Knuutila, K. Hedman, Lymphoproliferative disease after allogeneic stem cell transplantation–pre-emptive diagnosis by quantification of Epstein–Barr virus DNA in serum, J. Clin. Virol 28 (2003) 275–283.
[25] H.J. Brown, M.J. Song, H. Deng, T.T. Wu, G. Cheng, R. Sun, NF-kappaB inhibits gammaherpesvirus lytic replication, J. Virol 77 (2003) 8532–8540.
[26] J.M. Adams, Ways of dying: multiple pathways to apoptosis, In: Genes Dev, 17 (2003) 2481–2495.
[27] R. Horie, M. Watanabe, T. Okamura, M. Taira, M. Shoda, T. Motoji, A. Utsunomiya, T. Watanabe, M. Higashihara, K. Umezawa, DHMEQ, a new NF-kappaB inhibitor, induces apoptosis and enhances fludarabine effects on chronic lymphocytic leukemia cells, Leukemia 20 (2006) 800–806.

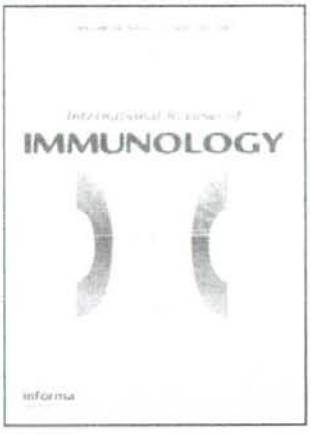

International Reviews of Immunology
Publication details, including instructions for authors and subscription information:
http://www.informaworld.com/smpp/title~content=t713643575

Potential Role of NK Cells in the Induction of Immune Responses: Implications for NK Cell-Based Immunotherapy for Cancers and Viral Infections

Hiroshi Terunuma [abc]; Xuewen Deng [a]; Zahidunnabi Dewan [d]; Shigeyoshi Fujimoto [a]; Naoki Yamamoto [d]
[a] Biotherapy Institute of Japan, Tokyo, Japan
[b] Tokyo Clinic Marunouchi Oazo mc, Tokyo, Japan
[c] Southern Tohoku Research Institute for Neuroscience, Fukushima, Japan
[d] AIDS Research Center, National Institute of Infectious Disease, Tokyo, Japan

Online Publication Date: 01 May 2008
To cite this Article: Terunuma, Hiroshi, Deng, Xuewen, Dewan, Zahidunnabi, Fujimoto, Shigeyoshi and Yamamoto, Naoki (2008) 'Potential Role of NK Cells in the Induction of Immune Responses: Implications for NK Cell-Based Immunotherapy for Cancers and Viral Infections', International Reviews of Immunology, 27:3, 93 - 110
To link to this article: DOI: 10.1080/08830180801911743
URL: http://dx.doi.org/10.1080/08830180801911743

International Reviews of Immunology, 27:93–110, 2008

ISSN: 0883-0185 print / 1563-5244 online
DOI: 10.1080/08830180801911743

informa
healthcare

Potential Role of NK Cells in the Induction of Immune Responses: Implications for NK Cell–Based Immunotherapy for Cancers and Viral Infections

Hiroshi Terunuma
Biotherapy Institute of Japan, Tokyo, Japan; Tokyo Clinic Marunouchi Oazo mc, Tokyo, Japan; and Southern Tohoku Research Institute for Neuroscience, Fukushima, Japan

Xuewen Deng
Biotherapy Institute of Japan, Tokyo, Japan

Zahidunnabi Dewan
AIDS Research Center, National Institute of Infectious Disease, Tokyo, Japan

Shigeyoshi Fujimoto
Biotherapy Institute of Japan, Tokyo, Japan

Naoki Yamamoto
AIDS Research Center, National Institute of Infectious Disease, Tokyo, Japan

Natural killer (NK) cells recognize tumor cells and virus-infected cells and attack without being sensitized to antigens. The development of the antitumor / antivirus activities of NK cells is controlled by multiple mechanisms such as direct cytotoxic activity against target cells, antibody-dependent cell-mediated cytotoxicity, secretion of Th1-type cytokines, and interactions with dendritic cells. The development of these activities plays a significant role in both innate and adaptive immunities. Considering the recent progress made in elucidating the molecular and cellular biology of NK cells, we summarize the current situation and discuss future possibilities with regard to NK cell–based adoptive immunotherapy.

Keywords adoptive immunotherapy, cancer immunotherapy, immunotherapy, NK cell, viral immunotherapy

Address correspondence to Hiroshi Terunuma, M.D., Ph.D., Biotherapy Institute of Japan, 2-4-8 Edagawa, Koutou-ku, Tokyo 135-0051, Japan. E-mail: terunuma_h@yahoo.co.jp

INTRODUCTION

Natural killer (NK) cells are lymphocytes that recognize tumor cells and infected cells and destroy them immediately without involving any specific antigen recognition mechanisms. Furthermore, they induce subsequent immune responses as the first-line immune cells of *in vivo* defense. At the present time, no single cell-surface marker for the identification of human NK cells has been determined, and detection of these cells is usually based on lymphocytes that are negative for CD3 and positive for CD16 or CD56. Although the ratio of NK cells varies according to age, sex, and so forth, these cells represent about 5–20% of peripheral blood lymphocytes in healthy adults.

During the past few years, many new findings have been reported in the field of the molecular and cellular biology of NK cells, including NK cell receptors, expression of major histocompatibility complex class I antigens on target cells, antibody-dependent cell-mediated cytotoxicity (ADCC), cross-talk with dendritic cells, and NK cell subsets as described in this review. In addition, we recently developed a feasible and safe method for *ex vivo* NK cell expansion. Based on these findings, the possibility of clinical use of NK cell–based adoptive immunotherapy is discussed.

NK Cell Receptors

NK cells were originally discovered as a group of cells with natural killing ability against tumor cells [1,2]. However, the mechanism by which NK cells recognize their target cells remained unknown for a long time. Kärre suggested the hypothesis of "missing self," in which NK cells are considered to recognize and attack tumor cells with decreased or absent expression of self-markers, namely major histocompatibility complex (MHC) class I molecules [3]. This hypothesis was proved at the molecular level in previous studies [4,5]. At the same time, it was clarified that not only a lack of inhibitory signals by missing-self molecules but also activating signals from the target cells are required for the recognition and killing action.

NK cells have many receptors, as summarized in Table 1. Many of these are paired receptors comprising activating and inhibitory receptors with similar extracellular domains but different functions. Inhibitory receptors have long intracellular domains with inhibitory signal motifs, whereas activating receptors have short intracellular domains and combine with adaptor molecules that possess signal motifs. The y chains of high affinity IgE receptors (FcεRIγ) and two killer cells activating receptor-associated proteins/DNAX-activating

TABLE I Human NK Cell Receptors

Receptor	Structure	Ligand	Adaptor	Signal type
CRACC	IgSF	CRACC	None	Activating
DNAM-1	IgSF	PVR, nectin-2	None	Activating
FcγRIII (CD16)	IgSF	IgG Fc region	FcεRIγ/CD3ζ	Activating
KIR2DL, KIR3DL	IgSF	HLA-A,B,C	None	Inhibitory
KIR2DS, KIR3DS	IgSF	Unknown	DAP12	Activating
LAIR-1	IgSF	Collagen	None	Inhibitory
LILR	IgSF	HLA-A,B,C,E,F,G	None	Inhibitory
NKp30 (CD337)	IgSF	Unknown	FcεRIγ/CD3ζ	Activating
NKp44	IgSF	Unknown	DAP12	Activating
NKp46 (CD335)	IgSF	Influenza HA	FcεRIγ/CD3ζ	Activating
NTB-4	IgSF	NTB-4	None	Activating
2B4 (CD244)	IgSF	CD48	None	Activating
KLRG1	C-lectin	Cadherins (E-,N-,R-)	None	Inhibitory
CD94-NKG2A	C-lectin	HLA-E	None	Inhibitory
CD94-NKG2C	C-lectin	HLA-E	DAP12	Activating
CD94-NKG2E	C-lectin	Unknown	DAP12	Activating
NKG2D	C-lectin	MICA/B,ULBP1-4	DAP10	Activating
NKR-P1	C-lectin	LLT	None	Inhibitory
NKR-PIA	C-lectin	LLT1	FcεRIγ/CD3ζ	Activating
LFA-1 (CD11a/CD18)	β2-integrin	ICAM-1,2,3,4	None	Activating

IgSF, immunoglobulin superfamily; HA, hemagglutin.

proteins of 12 kDa (DAP12) and 10 kDa (DAP10) have been identified as adaptor molecules. However, some activating receptors of NK cells do not require adaptor molecules, as the receptors themselves transmit the activating signals. Many of the inhibitory receptors ligate with MHC class I molecules. The paired receptors detect molecules expressed on the target cells and send activating or inhibitory signals for cytotoxic activity. The development of the cytotoxic activity of NK cells is then adjusted by the balance between the positive and negative signals transmitted inside the cells.

Once NK cells become activated, they damage the target cells through release of cytotoxic granules such as perforin or granzyme, expression of death-inducing ligands such as tumor necrosis factor–related apoptosis-inducing ligand (TRAIL) or FasL, and secretion of Th1-type cytokines or chemokines.

As mentioned above, many receptors have been identified on NK cells. This situation probably arises because NK cell receptors are encoded by embryonic genes, and numerous activating receptors are

required in order to maintain the variety in antigen recognition, unlike T-cell or B-cell receptors that create various patterns by random gene rearrangements.

In association with viral infections, NKp30, NKp44, and NKp46 have been identified as activating receptors that belong to the immunoglobulin superfamily. Although their ligands on tumor cells are still unknown, NKp44 and NKp46 have been reported to combine with influenza hemagglutinin and activate NK cells [6,7]. On the other hand, the activity of NKp30 is inhibited by ligation with pp65 of human cytomegalovirus, and this is an interesting escape mechanism for this virus from the immune system [8]. In HIV infection, the activating killer Ig-like receptor (KIR) allele KIR3DS1, in combination with human leukocycte antigen-B alles that encode molecules with isoleucinat at position 80 (HLA-B Bw4-80Ile) is associated with delayed progression to AIDS [9], whereas allelic combinations of KIR3DL1 and HLA-B Bw4 are associated with both AIDS progression and plasma HIV RNA abundance [10]. There are also ample indications that NK cells can eradicate malignant cells in patients with a favorable combination of HLA and KIR genes [11]. Selecting these individuals for specific treatments should provide insights into the feasibility of successful antitumor or antiviral therapy mediated through NK cells.

EXPRESSION OF MHC CLASS I MOLECULES ON TARGET CELLS

The balance between activating and inhibitory signals is important in the activation of NK cells. For this, the amounts of ligands expressed on the target cells are crucial, in addition to the amounts of activating and inhibitory receptors expressed on NK cells. Although tumor cells and virus-infected cells with decreased or absent MHC class I molecule expression can escape from attack by cytolytic T-lymphocytes (CTL), the cells are usually damaged by NK cells. As summarized in Table 2, many cases have been reported regarding tumor cells with downregulated or absent expression of MHC class I molecules. The frequency of loss or downregulation of MHC class I expression in metastatic tumors is higher than in the primary ones [12,13]. For the same types of tumor cases, the survival rate of patients is significantly low, and their relapse rate after treatment is significantly high [13,14]. Although certain tumors such as breast, colorectal, prostate, and cervical cancer have a high frequency of abnormal MHC class I expression, these types of tumors do not have the poorest prognosis. Further investigations are necessary to clarify how the level of NK cells and CTL activity in blood,

TABLE II Frequencies of Loss or Reduction in Expression of Major Histocompatibility Complex Class I Molecules in Surgically Removed Tumor Lesions

Tumor	Low or negative cases/total cases	Percentage (%)	Reference
Melanoma, primary	66/414	16	[12]
Melanoma, metastases	287/495	58	[12]
Head and neck carcinoma	20/41	49	[59]
Laryngeal carcinoma	25/70	36	[60]
Breast carcinoma	356/439	81	[61]
Lung carcinoma	35/93	38	[62]
Hepatocellular carcinoma	24/57	42	[63]
Colorectal carcinoma	63/87	72	[64]
Colorectal carcinoma, primary	144/455	32	[65]
Renal cell carcinoma	17/45	38	[14]
Bladder carcinoma	18/72	25	[66]
Prostatic carcinoma	311/419	74	[67]
Cervical carcinoma	27/30	90	[68]
Ovary carcinoma, primary	19/51	37	[69]
Bone and soft tissue sarcoma	46/74	62	[13]
Osteosarcoma, primary	13/25	52	[13]
Osteosarcoma, metastases	7/8	88	[13]

and the balance between activating and inhibitory ligands of NK cell receptors expressed on the surface of tumors, besides the level of MHC class I expression, contribute to the prognosis of each type of tumor.

On the contrary, T lymphocytes infected by HIV are not destroyed by NK cells, regardless of their abnormal expression of MHC class I molecules [15–17]. In such cases, expression of HLA-C or HLA-E, the ligands of inhibitory receptors, is hardly inhibited, although HLA-A or HLA-B expression is inhibited. Therefore, HIV-infected cells can escape from attack by CTL or NK cells [16–18]. It is necessary to clarify whether such cases also occur with tumor cells.

ADCC

NK cells not only work nonspecifically with antigens but also remove tumor cells and infected cells on which antigen-specific antibodies are bound by ADCC. This process occurs through the activating receptor CD16, which is also used to identify NK cells among lymphocytes. CD16 is a low-affinity activating Fc receptor that allows NK cells to interact with antibody-coated cells, thereby inducing ADCC as well as secretion of interferon (IFN)-γ, tumor necrosis factor (TNF)-α, or T-cell recruiting chemokines [19,20]. CD16 is expressed on monocytes, macrophages,